Analysis of an Electro-Thermal-Compliant Actuator

1. Basic electro-thermal actuator

Electro-thermal actuation in microsystems is based on a simple principle: passing electric current through a constrained elastic structure causes it to deform due to thermal loads created by Joule heating. Design of the structural dimensions and a good choice of material enable us to maximize the output stroke against a given load. Here, we consider a simple electro-thermal-compliant (ETC) actuator (see Fig. 1) proposed in [1, 2]. This planar structure is made of an electrically conducting material. Structurally, it can be broken down into four segments: 1) the narrow beam, 2) the connector, 3) the wide beam, and 4) the flexure. The proportions of the structure are shown in the figure. The out-of-plane thickness is $p_t L$. The left ends of the narrow beam and flexure are mechanically anchored and thermally grounded to the ambient temperature T_0. An voltage V is applied between them.

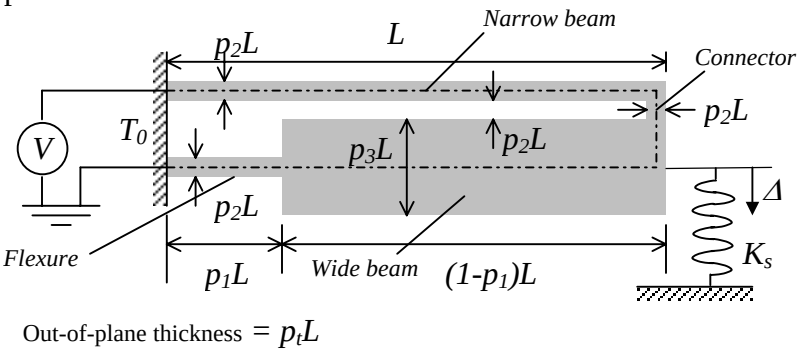

Fig. 1 Basic electro-thermal actuator

The actuator works as follows. When V is applied, an electric current J passes from end to end, and Joule heating ensues. Due to uneven cross-section area along this slender structure, the current density, and hence, Joule heating are nonuniform leading to a temperature distribution. Depending on the proportions, either the narrow beam or the wide beam expands more than the other. Since the narrow beam and the flexure bend more easily than the connector, this mismatch in axial thermal expansion of the two beams causes this constrained structure to deflect sideways in the downward or upward direction. In Fig. 1, this deflection is indicated by Δ downward at the right end of the wide beam. A mechanical spring of spring constant K_s, is shown attached to the output point. The spring simulates the output force from the structure attached to the actuator. For simplicity, we assume that the spring is insulated electrically and thermally.

For a given size-factor L and an voltage V, our objective is to determine the proportions $p_1, p_2, p_3,$ and p_t, and select the best material to maximize the output deflection Δ and to minimize the input electrical power such that the specified operating temperature is sufficiently far away from the melting point T_m of the material, and the maximum stress is sufficiently lower than the failure strength σ_f. Therefore, the following material properties are relevant to this

actuator: electrical resistivity (ρ_e), thermal conductivity (k_t), thermal expansion coefficient (α), melting point (T_m), failure strength (σ_f), and Young's modulus (E).

There are three steps in the analysis of the ETC actuator. The three steps can be carried out sequentially if we ignore the temperature-dependence of the material properties. First, an electrical analysis is needed to determine the current density in each of the four segments. Then, using the Joule heating, the temperature profile is to be determined. And, finally, the elastic analysis is to be done to compute the output deflection. For the sake of simplicity, we do not include the convection and radiation effects (see [3] where they were considered).

The slender segments in the structure make it easy to analyze it using a one-dimensional electrical and thermal analysis, and an Euler beam-based elastic analysis. The foregoing analytical modeling is a simplified version of the comprehensive treatment in [4].

2. Electrical analysis

The four segments in the actuator can be treated as electrical resistors in series. The resistance of an axial conductor of this type is given by the electrical resistivity times the length divided by the cross-section area. Thus, we have

$$R_i = \frac{\rho_e L_i}{A_i} \text{ for } i = 1,2,3,4 \tag{1}$$

Noting the relative proportions shown in Fig. 1, we get the combined series-resistance as

$$R = R_1 + R_2 + R_3 + R_4 = \frac{\rho_e}{L}\left\{\frac{1}{p_t p_2} + \frac{1}{p_t} + \frac{(1-p_1)}{p_t p_3} + \frac{p_1}{p_t p_2}\right\} = \phi_e \frac{\rho_e}{L} \tag{2}$$

The current J, and the electrical input power P_e are given by

$$J = \frac{V}{R} = \frac{LV}{\phi_e \rho_e} \tag{3}$$

$$P_e = J^2 R = \frac{LV^2}{\phi_e \rho_e} \tag{4}$$

The Joule heating per unit volume per unit time in each of the four segments, i.e., $\dot{Q}_{e_i}\,(i = 1 to 4)$, which acts as the heat source for the thermal analysis, can be written as follows using Eqs. (1) through (3).

$$\dot{Q}_{e_i} = \frac{J^2 R_i}{A_i L_i} = \frac{L^2 V^2}{\phi_e^2 A_i^2 \rho_e} \text{ for } i = 1,2,3,4 \tag{5}$$

i.e,

$$\dot{Q}_{e_1} = \frac{V^2}{\phi_e^2 p_t^2 p_2^2 L^2 \rho_e}$$
$$\dot{Q}_{e_2} = \frac{V^2}{\phi_e^2 p_t^2 p_2^2 L^2 \rho_e}$$
$$\dot{Q}_{e_3} = \frac{V^2}{\phi_e^2 p_t^2 p_3^2 L^2 \rho_e} \qquad (6)$$
$$\dot{Q}_{e_4} = \frac{V^2}{\phi_e^2 p_t^2 p_2^2 L^2 \rho_e}$$

3. Thermal analysis

The slender segments are amenable for axial heat conduction analysis. Since the connector segment is very short, the temperature distribution in it is neglected but the heat generated in it is taken into account in balancing the flux across its two interfaces. The temperature $T_i(x)$ in each of the three remaining segments is governed by the diffusion equation shown below.

$$\frac{d^2 T_i(x)}{dx^2} + \frac{\dot{Q}_{e_i}}{k_t} = 0 \text{ for } i = 1,3,4 \qquad (7)$$

where x runs from zero through the length of the respective segment. With convection and radiation neglected, the only boundary conditions at either end of each segment are either due to the temperature being equal to the ambient or the continuity of heat flux across the interface between two segments. The differential equation in Eq. (7) can be readily solved as

$$T_i(x) = -\frac{\dot{Q}_{e_i}}{2k_t} x^2 + a_i x + b_i \qquad (8)$$

where the constants a_i and b_i ($i = 1,3,4$) are solved using the following six boundary conditions:

1. Temperature at the left end is at the ambient temperature:

$$T_1(x = 0) = T_0 \text{, i.e., } b_1 = T_0 \qquad (9a)$$

2. Temperature at the right end of the narrow beam is equal to that at the right end of the wide beam:

$$T_1(x = L_1) = T_3(x = 0) \text{, i.e., } -\frac{\dot{Q}_{e_1}}{2k_t} L^2 + a_1 L + T_0 = b_3 \text{ which can be simplified as}$$

$$a_1 L - b_3 = \frac{\phi_{t_1} V^2}{\phi_e^2 \rho_e k_t} - T_0 = c_1 \text{ with } \phi_{t_1} = \frac{1}{2 p_t^2 p_2^2} \qquad (9b)$$

3. Continuity of heat flux across the connector along with the heat generated in it:

$$-k_t A_1 \left.\frac{dT_1}{dx}\right|_{x=L_1} - k_t A_3 \left.\frac{dT_3}{dx}\right|_{x=0} + \dot{Q}_{e_2} A_2 L_2 = 0 \text{ which can be simplified as}$$

$$-k_t p_t p_2 L^2 \left(-\frac{\dot{Q}_{e_1}}{k_t} L + a_1 \right) - k_t p_t p_3 L^2 a_3 + \dot{Q}_{e_2} p_t p_2^3 L^3 = 0$$

$$p_2 L a_1 + p_3 L a_3 = \frac{\phi_{t_2} V^2}{\phi_e^2 \rho_e k_t} = c_2 \text{ with } \phi_{t_2} = \frac{1}{p_t}\left(1 - \frac{1}{p_2}\right) \tag{9c}$$

4. Temperature at the left end of the wide beam is equal to that at the right end of the flexure:

$T_3(x = L_3) = T_4(x = 0)$, i.e., $-\frac{\dot{Q}_{e_3}}{2k_t}(1-p_1)^2 L^2 + a_3(1-p_1)L + b_3 = b_4$ which can be simplified as

$$(1-p_1)La_3 + b_3 - b_4 = \frac{\phi_{t_3} V^2}{\phi_e^2 \rho_e k_t} = c_3 \text{ with } \phi_{t_3} = \frac{(1-p_1)^2}{2p_t^2 p_3^2} \tag{9d}$$

5. Heat flux continuity across the interface between the wide beam and the flexure:

$$k_t A_3 \left.\frac{dT_3}{dx}\right|_{x=L_3} - k_t A_4 \left.\frac{dT_4}{dx}\right|_{x=0} = 0 \text{ which can be simplified as}$$

$$k_t p_t p_3 L^2 \left(-\frac{\dot{Q}_{e_3}}{k_t}(1-p_1)L + a_3 \right) - k_t p_t p_2 L^2 a_4 = 0$$

$$p_3 L a_3 - p_2 L a_4 = \frac{\phi_{t_4} V^2}{\phi_e^2 \rho_e k_t} = c_4 \text{ with } \phi_{t_4} = \frac{(1-p_1)}{p_t^2 p_3} \tag{9e}$$

6. Temperature at the left end of the flexure is at the ambient temperature:

$T_4(x = L_4) = T_0$, i.e., $-\frac{\dot{Q}_{e_4}}{2k_t} p_1^2 L^2 + a_4 p_1 L + b_4 = T_0$ which can be simplified as

$$p_1 L a_4 + b_4 = \frac{\phi_{t_5} V^2}{\phi_e^2 \rho_e k_t} + T_0 = c_5 \text{ with } \phi_{t_5} = \frac{p_1^2}{2p_t^2 p_2^2} \tag{9f}$$

Eqs. (9b) through (9f) can be solved for $\{a_1, a_3, b_3, a_4, b_4\}$. Notice that, for consistency, $b_i s$ should have units of temperature, and $a_i s$ temperature per unit length. Thus, in view of Eq. (8), the temperature profile depends on the material properties and relative proportions but not on the size-factor, L. Furthermore, the maximum temperature can be expressed as follows.

$$T_{\max} = \phi_{t\max} \frac{V^2}{\rho_e k_t} \tag{10}$$

where $\phi_{t\max}$ is a non-dimensional quantity that depends on the relative proportions of the dimensions of the structure.

4. Elastic analysis

Just as in electrical and thermal analyses, slenderness of the segments in the ETC actuator makes it possible to use Euler beam theory to analyze the elastic deflections under the thermal loads. The purpose of this analysis is to derive analytical expressions for the output deflection Δ, and maximum stress, $\sigma_{\max}$. The deflection Δ can be determined as follows using Maizel's theorem (see [5 or 4] for a derivation):

$$\Delta = \sum_{i=1}^{4} \left[\int_0^{L_i} \hat{F}_{axial_i}(x)\, \alpha \left\{ T(x)_i - T_0 \right\} dx \right] \tag{11}$$

where $\hat{F}_{axial_i}(x)$ is the axial force induced in the i^{th} segment due to a unit force applied at the output in the desired output direction for given mechanical boundary conditions including the output spring but in the absence of thermal loading. Upon integration of Eq. (11), we get

$$\Delta = \phi_\Delta V^2 L \frac{\alpha}{\rho_e k_t} \tag{12}$$

where ϕ_Δ is a non-dimensional quantity that depends on the relative proportions of the structure and the output spring constant, K_s. Notice the absence of Young's modulus in this expression. This is because thermal load causes a *strain* and a *force* wherein the deflection is not altered by the material's intrinsic stiffness. It is also clear from the dimensional analysis of Eq. (11).

The derivation of the analytical expression for maximum stress is cumbersome. But, noting that the stress here is caused by thermal strain, which is $\alpha(T - T_0)$, we can conjecture that the maximum stress in the structure is proportional to $E\alpha(T - T_0)$. Therefore, it has the following form.

$$\sigma_{\max} = \phi_{s\max} V^2 \frac{E\alpha}{\rho_e k_t} \tag{13}$$

where $\phi_{s\max}$ is a non-dimensional quantity that depends on the relative proportions of the structure and the output spring constant, K_s.

References

1. Guckel, H., Klein, J., Christenson, T., Skrobis, K., Laudon, M., and Lovell, E.G., "Thermo-Magnetic Metal Flexure Actuators," *Technical Digest of the Solid State Sensors and Actuators Workshop*, Hilton Head Island, SC, 1992, pp. 73-75.
2. Comtois, J. and Bright, V., "Surface Micromachined Polysilicon Thermal Actuator Arrays and Applications," *Technical Digest of the Solid-State Sensors and Actuators Workshop*, Hilton Head Island, SC, 1996, p. 174.

3. Mankame, N. and Ananthasuresh, G.K., 2001, "Comprehensive Thermal Modeling and Characterization of an Electro-Thermal-Compliant Microactuator," *Journal of Micromechanics and Microengineering*, **11**, No. 5, (2001), pp. 452-462.
4. Mankame, N., 2000, "Modeling of Electro-Thermal-Compliant Micromechanisms," *Masters thesis*, University of Pennsylvania.
5. Kovalenko, A, 1969, *Thermoelasticity—Basic Theory and Applications*, Walters-Noordhoff Publishing, Groningen, The Netherlands.